Korean J. Chem. Eng., 36(9), 1421-1431 (2019)
DOI: 10.1007/s11814-019-0328-5

pISSN: 0256-1115
eISSN: 1975-7220

Ethylenediamine/glutaraldehyde-modified starch: A bioplatform for removal of anionic dyes from wastewater

Niyaz Mohammad Mahmoodi*,†, Mahdieh Sadat Mirmohammad Ali Roudaki, Khadijeh Didehban**, and Mohammad Reza Saeb*****

*Department of Environmental Research, Institute for Color Science and Technology, Tehran 1668814811, Iran
**Department of Chemistry, Payame Noor University, Tehran, Iran
***Department of Resin and Additives, Institute for Color Science and Technology, P. O. Box: 16765-654, Tehran, Iran
(*Received 10 December 2018 • accepted 19 June 2019*)

Abstract−The worth of this work lies in giving the surface of starch a positive charge for removal of azo dyes. A novel ethylenediamine/glutaraldehyde-modified starch (SEG) bioadsorbent was developed here, characterized by Fourier infrared spectroscopy and scanning electron microscopy analyses, and then applied in removal of Direct Red 23 (DR23) and Acid Blue 92 (AB92) anionic dyes from aqueous solutions. The efficacy of the SEG as bio-based adsorbent was studied in terms of adsorption characteristics, including dye removal percent, adsorption capacity, adsorption kinetic and adsorption isotherm, taking the initial dye concentration, adsorption time and SEG dosage as changing variables. Overall, it was found that the SEG is an efficient bio-based adsorbent in removal of anionic dyes. Experimental analyses (Temperature=25 °C & pH=2) revealed that either a pseudo-second-order kinetic or Langmuir isotherm model can properly express the behavior of adsorption based on chemisorption phenomenon. For structural change characterization, FT-IR analysis was performed. The highest adsorption efficiency belonged to the solution in which 0.035 g SEG was added to 30 mg/L water.

Keywords: Starch, Anionic Dyes, Adsorption, Dye Removal, Adsorption Kinetic, Isotherm

INTRODUCTION

Several methods, such as photocatalysis and adsorption, were found to be effective, as well as cheap for dye removal. Albeit with some exceptions, activated carbon based adsorbents were found to be the best choices for dye removal from industrial wastewater effluents, but their cost restricts their use at large scale uses. The use of non-conventional dye removal methods in the lab provides investigators with a general basis for future trials in the quest for cheap yet high efficiency adsorbents from natural candidates. Interest in using adsorbents for removal of organic pollutants from wastewater and water resources has steadily grown in recent years [1-8]. In this sense, the use of natural biopolymer adsorbents such as starch, chitosan, and alginate has been extensively recommended [9-12]. As the second low-cost biodegradable natural resource after cellulose, starch has been widely applied in diverse fields such as medicine, agriculture, and packaging industry [13-17]. Besides being abundant in nature, starch has a low cost, but high biodegradability, high reactivity and chemical stability thanks to the presence of reactive hydroxyl groups in its structure, which makes it a good candidate for adsorbent applications [18-21]. In the form of branched homopolymers of glucose, starch appears as a polysaccharide composed of linear long chains of amylose (10-30%) and highly branched backbone of amylopectin (70-90%) [22-26], which is characteristic of reactive adsorbents.

The use of polysaccharides of cellulose, chitosan and starch as adsorbent has received more attention in recent years in view of their biocompatibility and biodegradability [27-30]. It provides the user with an excellent selectivity towards aromatic compounds and metals—the reason why it has the potential for chemical interaction with a wide variety of molecules [31]. Nevertheless, poor physical properties of starch, including low mechanical properties and limited dimensional stability, place limits on the use of starch [31-33]. Chemical modification of starch gives this natural material the potential for removal of pollutants from wastewater [34-36]. Removal of diverse synthetic dyes or metal ions from textile and industrial wastewaters could be considered as a hot area in which starch plays the role of adsorbent, even in small amounts, to eliminate synthetic dyes from the ecosystem [37-39].

Diverse adsorption techniques, including coagulation/flocculation, membrane filtration, and oxidation, have been applied for removal of dyes and color pollutants from chemical company wastewater [40-42]. Biodegradation and biological decolorization have received more attention in recent years for removal of dyestuffs [43]. The use of agricultural wastes and polysaccharides adsorbent has also been practiced in dye removal thanks to their low cost and acceptable adsorption abilities [25,44]. For instance, over an isotherm temperature interval and by fitting model expressing kinetics, it was found that cationized starch-based adsorbents are promising in removal of Acid Blue 25 from aqueous solutions [38,45]. There is agreement that generation of negatively charged groups in the

†To whom correspondence should be addressed.
E-mail: mahmoodi@icrc.ac.ir, nm_mahmoodi@aut.ac.ir, nm_mahmoodi@yahoo.com

starch-based adsorbents can strongly increase their interaction with the positive charges from organic dyes [46]. However, the use of modified starch with high removal ability towards inherently positively charged dyes has been rarely addressed in the literature.

The focus of this work is on surface modification of starch with ethylenediamine/glutaraldehyde and applying it as a bioplatform in removal of two kinds of azo dyes, namely Acid Blue 92 (AB92) and Direct Red 23 (DR23), from wastewater. Since the surface of starch has a negative nature, it was attempted to make it positive to use it for removal of azo dyes. Surface characterization of starch was viewed by Fourier transform infrared (FTIR) spectroscopy, while its surface topology was observed by scanning electron microscopy (SEM) before and after dye adsorption on ethylenediamine/glutaraldehyde-modified starch (SEG). Dye removal, adsorption capacity, and kinetics of adsorption were measured by different isotherm models to find the best model imitating adsorption capacity of as-received and surface-modified starch towards AB92 and DR23 as a function of temperature, initial dye concentration in model wastewater, adsorbent dosage and pH. The main advantage of the developed adsorbent over previously reported starch-based adsorbents is its fast adsorption kinetics that follow the pseudo-second order model working on the basis of chemisorption phenomenon.

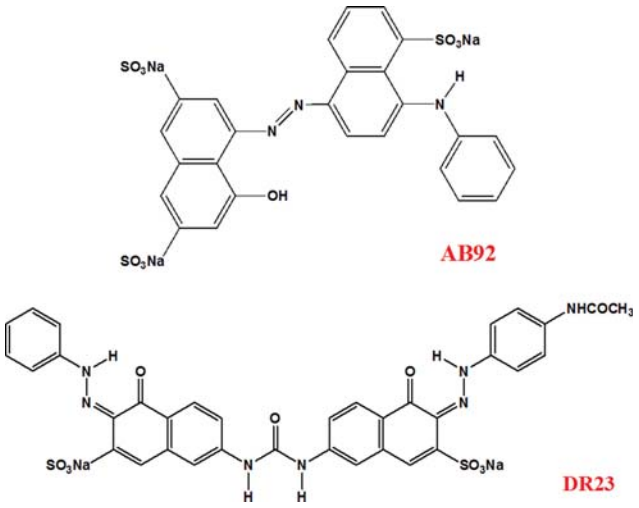

Fig. 1. Chemical structure of AB92 and DR23 azo dyes used in this study.

MATERIALS AND METHODS

1. Material

Starch in the form of powder was provided by Merck Chemical Co. (Germany). Ethylenediamine, glutaraldehyde, and HCl 37% (for PH adjustment) were similarly purchased from Merck. AB92 (λ_{max}=588 nm) and DR23 (λ_{max}=507 nm), with chemical structures shown in Fig. 1, were provided from local market. Distilled water was utilized in preparing solutions containing different types and concentrations of dyestuffs.

2. Synthesis of SEG

First, 2 g of starch was weighed and transferred into a 100 mL vessel. Then, 1 mL ethylenediamine and 1 mL glutaraldehyde were concurrently added dropwise into the container. The reaction between the amino groups attached to the surface of starch and the aldehyde groups of glutaraldehyde took place in the aqueous solution. The mixture was then continued for 14 h at 70 °C to assure reaction completion. Fig. 2 displays a very ideal molecule which we were wishing for, but we can hardly accept that grafting and cross-linking could take place so perfectly. The resulting powder, SEG, was washed several times with distilled water, dried at 80 °C for 24 h, and eventually collected for dye removal.

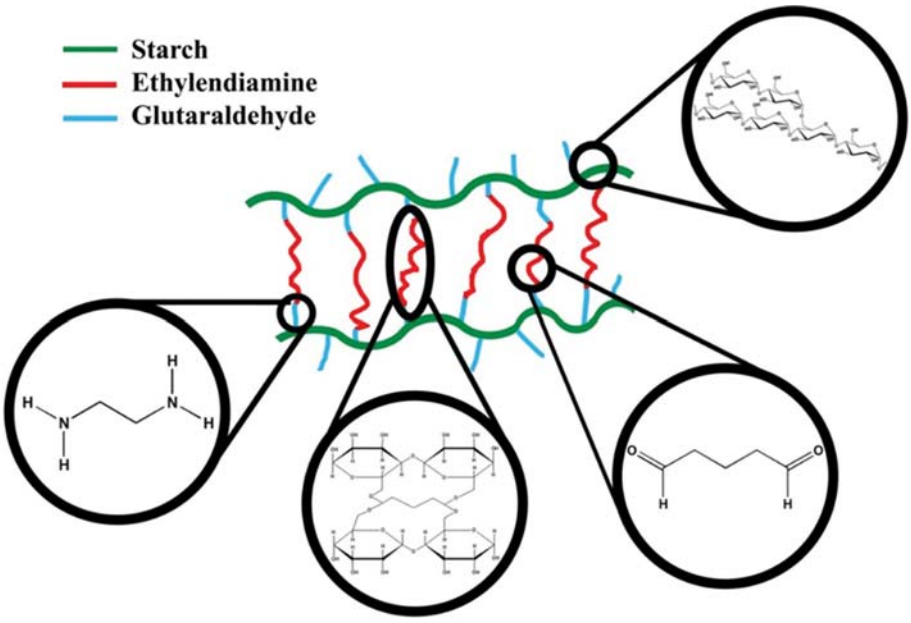

Fig. 2. Ideal view of SEG molecule from an optimistic viewpoint.

3. Adsorption of AB92 and DR23 Using the Modified Starch

The batch experiments were performed using 250 mL beaker with different amounts of SEG and 200 mL azo dyes (AB92 and DR23 solutions with different adsorbent dosage) for 1 hour at room temperature under magnetic stirring (300 rpm). The amount of dyes adsorbed on SEG bioplatform surface was accordingly measured at specified times. The effects of pH of solution, the contact time and the initial concentration of adsorbent on the adsorption efficiency were consequently studied. The mixtures were centrifuged under 5,800 rpm speed for 10 min, and the residual concentration of AB92 and DR23 dyes remained in the solution was determined according to the calibration curve by a UV-Vis spectrophotometer (Cecil 2021) at 588 nm and 507 nm, respectively. The adsorption capacity and dye removal efficiency of samples were calculated by the following equations:

$$q_t = \frac{C_0 - C_e}{W} \times V \quad (1)$$

$$\text{Removal efficiency } (\%) = \frac{C_0 - C_e}{C_0} \times 100 \quad (2)$$

where q_t is the adsorption capacity in the adsorbent at equilibrium (mg/g), C_0 is the initial dye concentration in the solution (mg/L), C_e is the equilibrium dye concentration at any time t (mg/L), V is the volume of solution (L), and W is the weight of the adsorbent used (g).

4. Characterization

The concentration of the AB92 and DR23 in the solution was measured utilizing a UV-Vis spectrophotometer (Cecil 2021) at 588 and 507 nm according to the calibration curves. Fourier transform infrared (FTIR) spectra of the pristine starch and SEG (or modified starch), were collected on a Matson FTIR spectrophotometer working in the range of 400-4,000 cm^{-1} using the KBr pellet method. A field-emission scanning electron microscope (FE-SEM; Mira TESCAN) working at an accelerating voltage of 15 kV was also utilized to observe the morphology of powders as well as surface

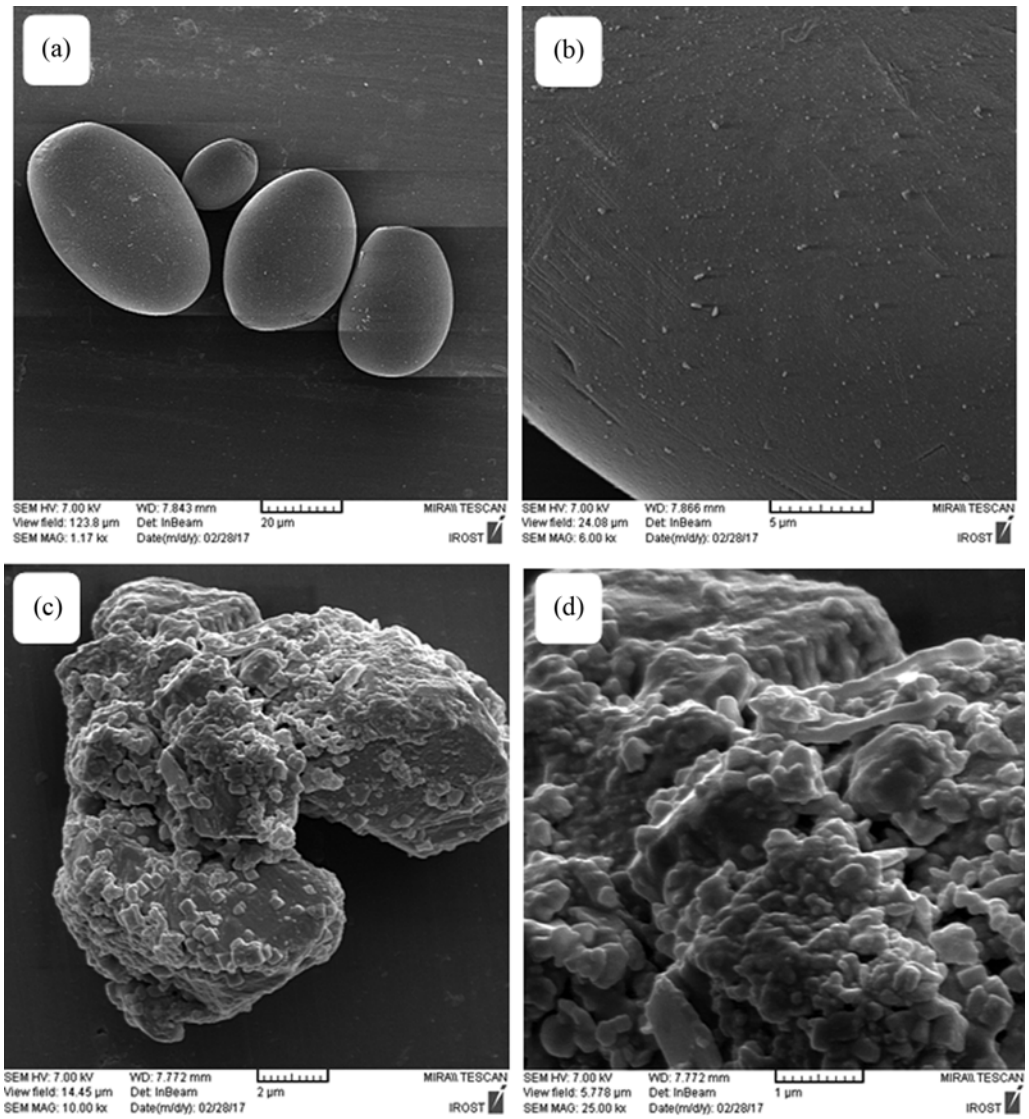

Fig. 3. FE-SEM micrographs of (a) starch granules, (b) starch granules at higher magnification, (c) SEG and (d) SEG at higher magnification.

of adsorbents before and after adsorption.

RESULTS AND DISCUSSION

1. Structural and Surface Morphology Analyses

The morphology of pristine starch and SEG was observed by FE-SEM technique. Fig. 3(a) shows granules of starch in elliptical shape different in size. A closer view of the lateral surface of particles is shown in Fig. 3(b). It is evident that the surface morphology of starch was clearly changed by modification with ethylenediamine/glutaraldehyde. Moreover, Fig. 3(c) and Fig. 3(d) show the amorphous irregular structure of the SEG obtained in different magnifications.

Fig. 4 shows SEM micrographs of SEG after azo dyes were adsorbed on it. It can be seen the spherical shape of SEG adsorbent remained unchanged, and no obvious conclusion can be drawn from comparison between AB92- and DR23-adsorbed SEG. This highlights the need for further investigations to infer the sufficiency of SEG adsorbent from chemical bonding and chemical kinetics points of view.

2. FTIR Analyses

The FTIR spectra were used to probe into functional groups attached to the surface of starch after functionalization through comparison between pristine starch and SEG (Fig. 5). The characteristics broad peaks appeared at 3,428 and 3,414 cm^{-1}, respectively, corresponding to as-received starch and SEG, can be corresponded to O-H stretching vibration of polymeric compounds, while the one at 2,932 cm^{-1} represents the presence of -CH_3 [47]. Since the peak of N-H of primary amine normally appears in the interval of 3,350-3,310 cm^{-1}, it was difficult to detect and assign such a peak to surface functionalization effect. It was also possible to have overlapping of N-H, C-H, and O-H stretching in the aforementioned zone [48]. The two peaks at 1,467 and 1,385 cm^{-1} are also assigned to the -CH bending vibration, whereas the ones observed at 1,654 and 859 cm^{-1} show the first and third overtone C-H stretching, respectively. Moreover, the bands at 1,160 and 763 cm^{-1} are attributed to the asymmetric and symmetric C-O-C stretching vibration, respectively [49]. The FTIR spectrum of the SEG shows some new bands indicative of the presence of amine groups on the surface of starch. The bands at 2,886 and 2,885 cm^{-1} are related to asymmetric and symmetric N-H stretching, respectively. Furthermore, the peaks observed at 812 and 861 cm^{-1} can be attributed to the out-of-plane N-H bending vibrations and C=N stretching vibration, respectively. The peak at 1,654 cm^{-1} for pristine starch can be related to the adsorbed moisture water content of pristine starch. On the other hand, looking at SEG spectrum suggests that

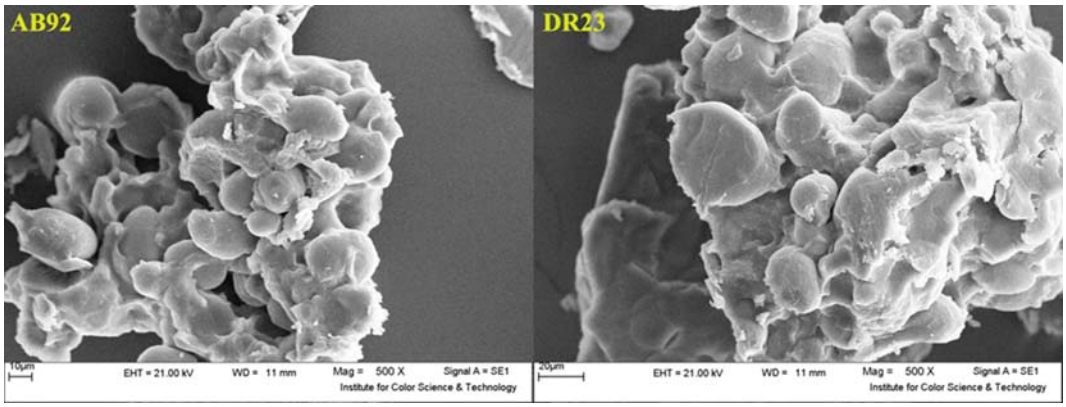

Fig. 4. FE-SEM micrographs of AB92 and DR23 adsorbed on SEG platform.

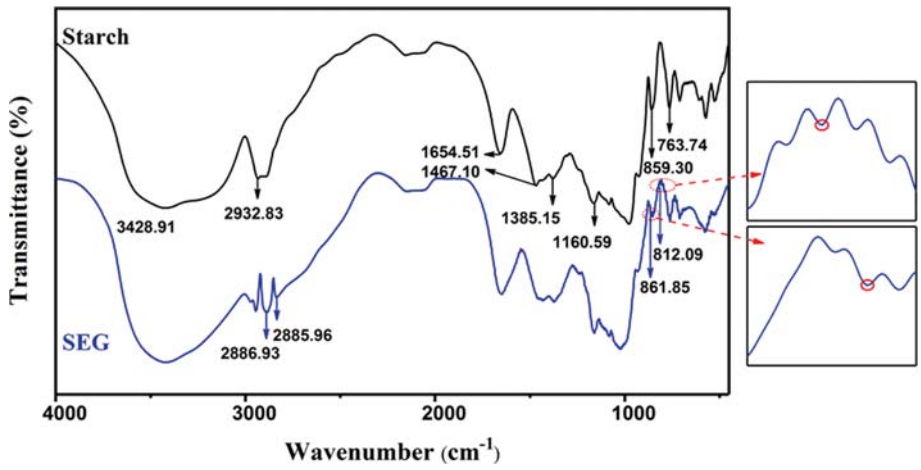

Fig. 5. FTIR spectra of the pristine and SEG-modified starch applied in this study.

the peak in the assigned region is broadened with a slight shift in the range from 1,690 to 1,640 cm^{-1}, which can be ascribed to the imide bond formed during the crosslinking amine and aldehyde groups.

FTIR spectra of AB92 and DR23 dyes in the as-received form and after being adsorbed on SEG are provided in Fig. 6. The band at ca. 2,920 cm^{-1} in AB92 FTIR spectrum has been intensified in the spectrum of SEG-modified starch, demonstrating the presence of this dye on the surface of adsorbent, as reflected in C-H hydrogen bonds. Moreover, the peak at 1,738 cm^{-1} ascribed to C=O carbonyl group was significantly brushed up in case of SEG on which AB92 was adsorbed, which was further approved around 1,035 cm^{-1} through broadening. In case of DR23, a peak at 2,965 cm^{-1} was observed in SEG adsorbed DR23 spectrum, which means that DR23 was removed by the SEG from model wastewater. The peak at 1,017 cm^{-1} was also due to C-O stretching, which was strongly affected by adsorption onto SEG-modified starch.

3. UV-Vis Analysis

The UV-Vis spectra of DR23 and AB92 show main bands representing maximum wavelengths at 507 and 588 nm, respectively (Fig. 7). The sudden fall in adsorption peaks of DR23 and AB92 at the assigned maxima suggests a fast removal of the anionic azo dyes.

4. Effect of pH of Solution

It is well-known that the pH of aqueous solution affects the adsorption efficiency of the adsorbent. In the case of starch, the capacity of adsorption was increased from 8 mg/g (for cationic dyes) to 167 mg/g (for anionic dyes) as the pH of the solution decreased from 5.0 to 2.0. From the lesson learned by the pH analysis, all the experiments were performed at pH acidity of 2.0 adjusted by a 2 N HCl solution. Surface treatment of starch changed its adsorption capacity, where a cationic nature was given to starch upon decreasing pH value, which gave the starch potential for removal of anionic dyes. At a lower pH, more NH_3^+ groups would present on the surface of SEG adsorbent with considerable tendency towards anionic dyes [22,44,50].

5. Effect of Contact Time, Adsorbent Dosage and Initial Concentration of Solution

Time-dependent dye removal percent and adsorption capacity of the SEG bioplatform as a function of SEG dosage at ambient temperature and acidic pH of 2.19 for DR23 and AB92 dyes are shown in Fig. 8 and Fig. 9, respectively. Overall, a fast adsorption was detected for both AB92 and DR23 during the first quarter of

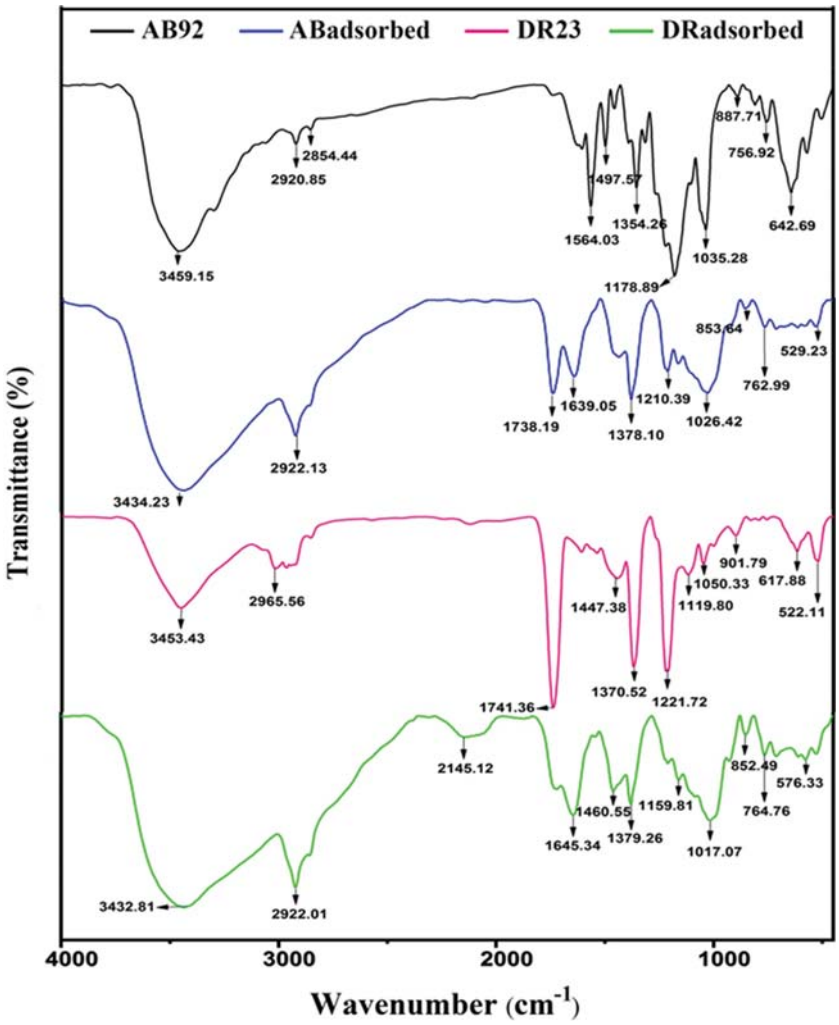

Fig. 6. FTIR spectra of AB92 and DR23 dyes in the pristine form and after being adsorbed onto SEG-modified starch.

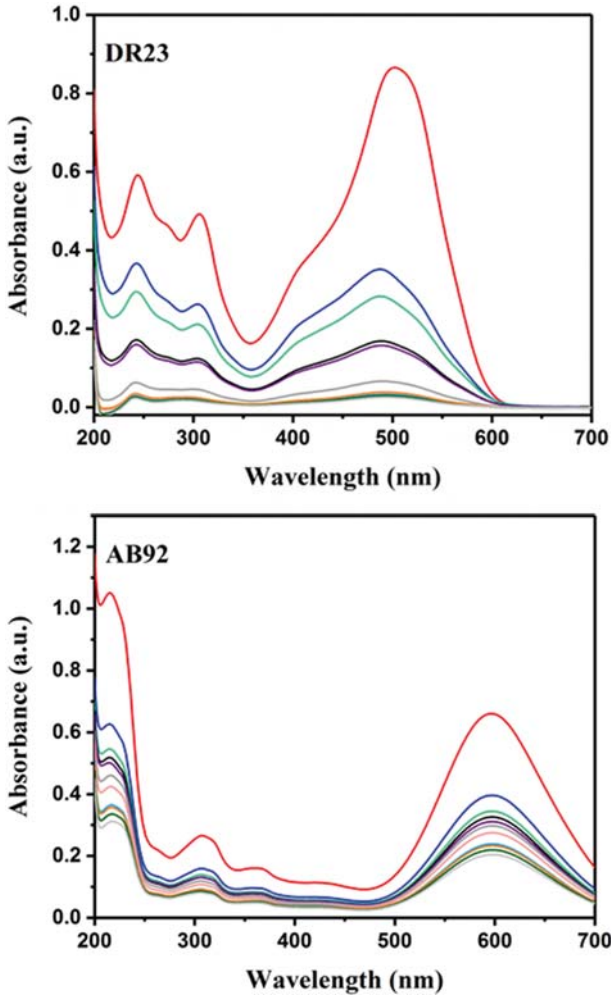

Fig. 7. UV-Visible adsorption spectra of DR23 and AB92 on SEG. Adsorbent dosage: 0.035 g, concentration: 30 mg/L, pH: 2.19 at room temperature.

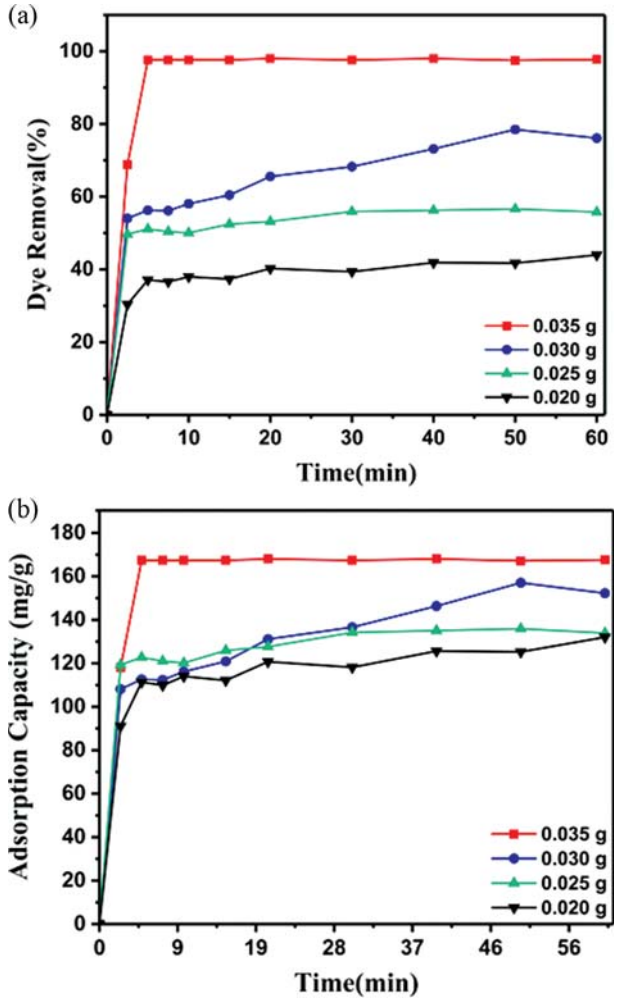

Fig. 8. Effect of contact time on (a) dye removal and (b) adsorption capacity of SEG towards DR23 at different adsorbent dosages and constant pH of 2.19 at ambient temperature.

exposure, then the adsorption experienced as equilibrium state until the end of test after 1 hour. Moreover, increase of adsorbent concentration in the solution caused increase in both removal percent and sorption efficiency towards DR23. On the other hand, adsorption capacity of SEG adsorbent towards DR23 was limitedly improved upon increase of SEG dosage. The availability of exchangeable sites from SEG at higher dosages of SEG adsorbent could be a reason behind this observation [51]. Moreover, the presence of amino groups on the surface of adsorbent as well as the nature of the dye could play a key role in determining the adsorption capacity [52]. There is also some evidence that starch may appear with a different character under various circumstances. Accordingly, a modification route has its own impacts on adsorption capacity of the starch-based sorbents. For instance, it was reported that crystalline regions in the starch structure are supposed to be converted into amorphous regions during acid-catalyzed hydrolysis of starch, where the enzyme in the starch can be depolymerized [53]. Moreover, starch is potent to be converted into its constituent, glucose in the presence of water through bifunctional mechanisms.

Since SEG was synthesized in the absence of hydrolysis or ethanol, a mono-functional mechanism would describe well the adsorption of dyes, where SEG might remain active during the test. Introduction of SEG to the aqueous solution of dyes could lead to a rise in dye removal capacity of adsorbent towards, but in an opposite manner would deteriorate reaction by increasing the concentration of adsorbent in an acidic media (Fig. 10). The surface of adsorbent suffers from a repulsive force between OH^- groups attached to the surface of starch and negative charges contributing from dyes in the solutions. This may unavoidably lead to a greater tendency between starch and amine groups in the case of AB92 anionic dye.

6. Adsorption Kinetics

6-1. Analysis of Kinetics of Dye Removal

The kinetic parameters of adsorption provide useful information to be applied in design of adsorption processes as well as prediction of adsorption efficacy [37,54]. The kinetics of adsorption using the developed SEG natural adsorbent was analyzed to give rise to a mechanistic description of AB92 and DR23 removal by the SEG from aqueous phase. Inspired by previous investigation of this group, two kinetic models of pseudo-first- and pseudo-sec-

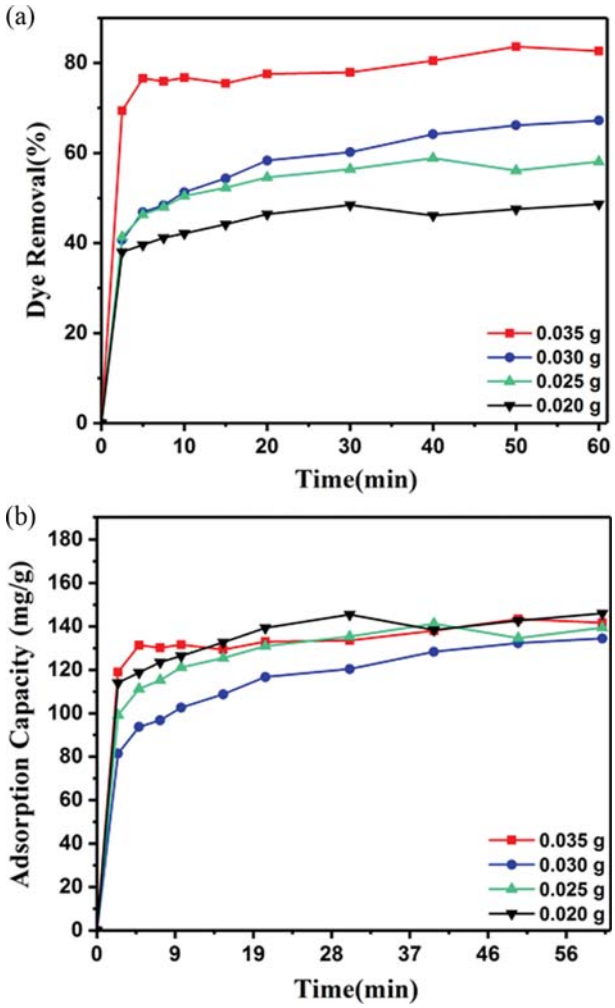

Fig. 9. Effect of contact time on dye removal (a) and adsorption capacity, (b) of the SEG towards AB92 at different adsorbent dosages and constant pH of 2.19 at ambient temperature.

ond-order were utilized for the analysis of experimental data. The linearized pseudo-first- and pseudo-second-order kinetic models are described through Eqs. (3) and (4), respectively:

$$\ln(q_e - q_t) = \ln q_e - k_1 t \tag{3}$$

$$\frac{t}{q_t} = \frac{1}{k_2 q_e^2} + \frac{t}{q_e} \tag{4}$$

In the above equations, the q_e and q_t, respectively, stand for the adsorption capacity of dyes (mg/g) at equilibrium and at time t (min), while k_1 (1/min) and k_2 (g/mg min) are, respectively, the pseudo-first- and pseudo-second-order rate constants. Normally, at low concentrations, e.g., 15 mg·L^{-1}, adsorption capacity and dye removal efficiency were both increased quickly after 10 min. After such a trial, the initial concentration of SEG was changed to mg/L to track its ability for dye removal. It was because fast adsorption of pollutants from wastewater is a very important factor determining the properness of the adsorbent in practical applications [22].

Fig. 11 and Fig. 12 show the kinetics behavior, while Table 1 gives detailed statistics of adsorption kinetics. The correlation coefficient (r^2) value of pseudo-first-order kinetic model was very poor (0.1516), while pseudo-second-order model with r^2 of 0.9998 could properly state adsorption capability of SEG adsorbent for removal of anionic AB92 and DR23 azo dyes from contaminated solutions. The main advantage of the pseudo-second order model lies in its fast adsorption kinetics based on the chemisorption phenomenon [46]. There are reliable reports to revise error analyses [55,56], but the linear least-squared method is a very simple way applied in analysis of kinetics data to give a wide spectrum of readers the sense that they can simply judge the worth of kinetic models when using linear methods.

As in Table 1, the $q_{e,cal}$ calculated using pseudo-second-order model matches closely with the experimental value ($q_{e,exp}$) (167.57 very close to 169.49 for DR23; and 141.17 very close to 142.86 for AB92 obtained at SEG dosage of 0.035 g). Thus, adsorption behav-

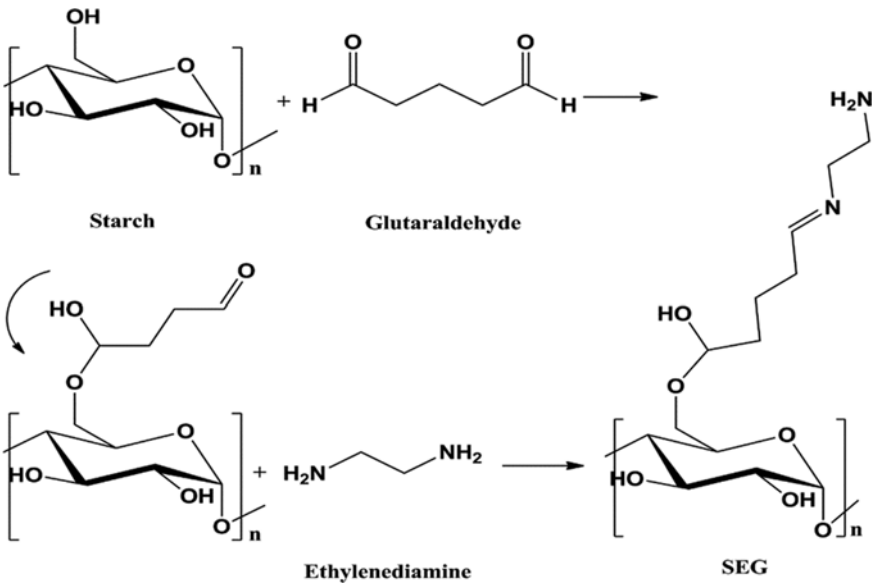

Fig. 10. Suggested mechanism for performance of SEG-modified starch.

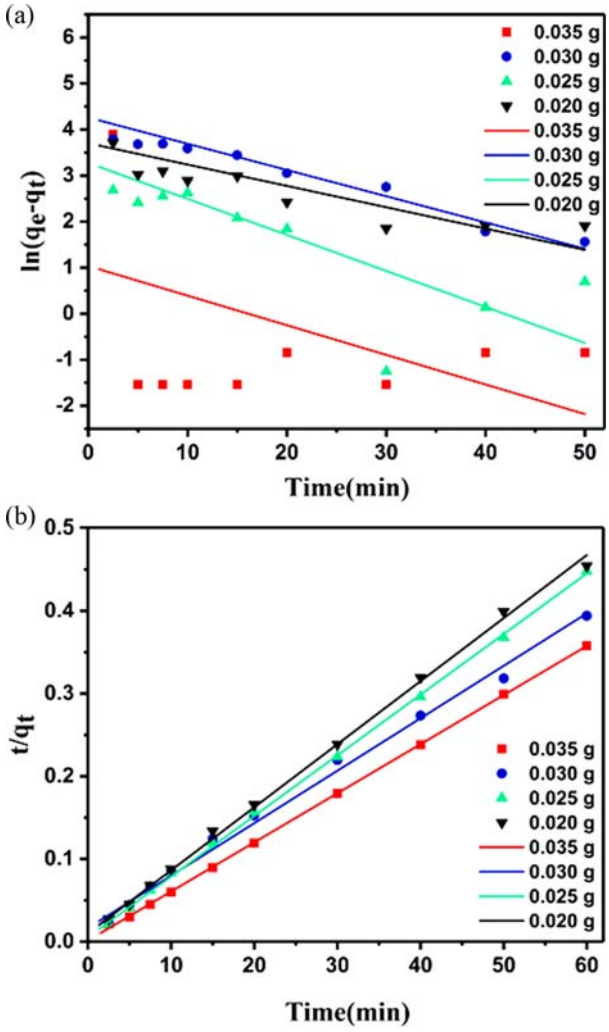

Fig. 11. Pseudo-first-order (a) and pseudo-second-order, (b) models applied in adsorption kinetics evaluation of DR23 (30 mg/L) onto SEG at pH of 2.19 and room temperature.

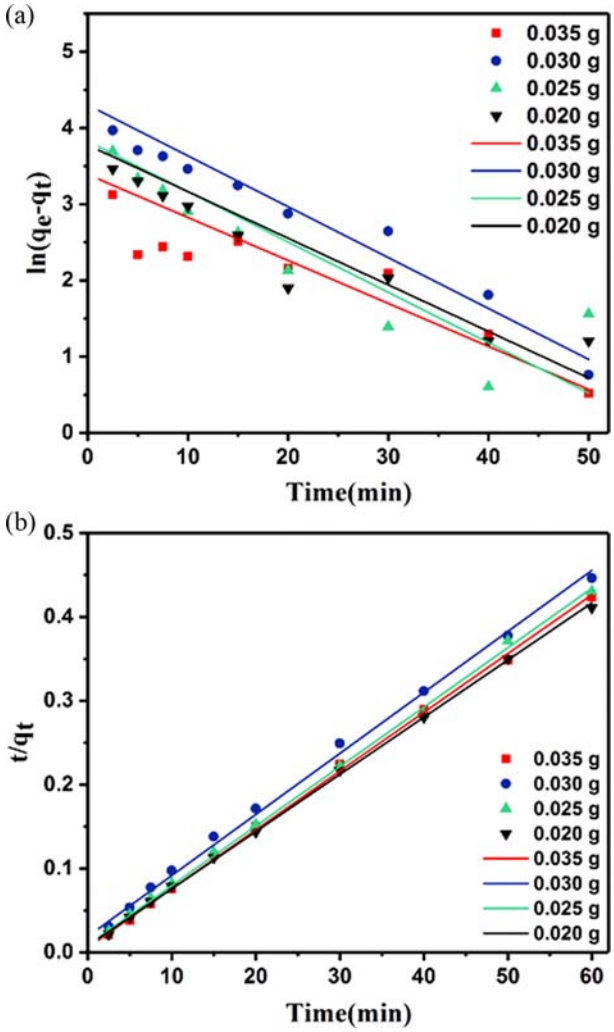

Fig. 12. Pseudo-first-order (a) and pseudo-second-order, (b) models applied in adsorption kinetics evaluation of AB92 (30 mg/L) onto SEG at pH of 2.19 and room temperature.

Table 1. Statistics of pseudo-first- and pseudo-second-order models applied for DR23 and AB92 elimination from wastewater by SEG

SEG dosage		Pseudo-first-order			Pseudo-second-order		
	$q_{e(exp)}$	$q_{e(cal)}$ (mg/g)	k_1 (min^{-1})	R^2	$q_{e(cal)}$ (mg/g)	k_2 (g/(mg min))	R^2
			DR23				
0.035	167.571	10.85425449	0.1480829	0.1923	169.4915254	0.023206667	0.9998
0.030	152.257	18247.35831	0.131271	0.9006	161.2903226	0.001875122	0.9949
0.025	133.907	1888.426125	0.1800946	0.6216	136.9863014	0.008074242	0.9995
0.020	132	5043.128103	0.1066289	0.6961	131.5789474	0.0046208	0.9984
			AB92				
0.035	141.169	2854.959817	0.1448587	0.7189	142.8571429	0.006712329	0.9989
0.030	134.46	20081.67804	0.1536101	0.941	138.8888889	0.002187342	0.9978
0.025	139.39	7239.357102	0.1639736	0.7607	142.8571429	0.004537037	0.9989
0.020	145.95	5985.494003	0.1407133	0.8035	147.0588235	0.004867368	0.9995

ior could be reliably simulated by a pseudo-second-order model, assuming that chemisorption was the mechanism explaining the interaction between SEG adsorbent and DR23 or AB92 dyes, which has been noticed *via* valence force acting to exchange electrons

between the adsorbent and the adsorbed specimen [46].

7. Adsorption Isotherms

Adsorption isotherms describe how an adsorbent can interact with an adsorbent. Such interactions are principally described by the Langmuir and Freundlich isotherms, where an optimized amount of adsorbent could be utilized. Thus, adsorption isotherms help to establish a relationship between the amount of dye adsorbed by the adsorbent and the amount of dye in the solution under an equilibrium condition [57]. The Langmuir isotherm works under the assumption that adsorption takes place in a monolayer onto the adsorbent surface with a fixed number of adsorption sites homogenously distributed in the adsorption area. It is also assumed that each site is able to adsorb only one molecule. Thus, all adsorption sites have the same value, and there is no interaction between adsorbates. On the other hand, the Freundlich isotherm describes the adsorption process on an amorphous surface considering the possible formation of various monolayers [46]. Therefore, it can be used for non-ideal adsorption in a heterogeneous system [57]. Since these models are successful in describing isotherms of adsorption, they were applied in this study to fit the experimental data. The Langmuir and Freundlich isotherms can be expressed by Eqs. (5) and (6), respectively:

$$\ln q_e = \ln K_f + \frac{1}{n}\log C_e \tag{5}$$

$$\frac{C_e}{q_e} = \frac{1}{K_L q_m} + \frac{C_e}{q_m} \tag{6}$$

where q_e stands for the adsorption capacity (mg/g) at equilibrium state and q_m is the maximum adsorption capacity (mg/g), C_e is the equilibrium concentration in the solution (mg/L), k_L is the Langmuir constant (L/mg), k_f is Freundlich constant (L/g) and the dimensionless parameter 1/n is the intensity of adsorption on the surface heterogeneity.

As shown in Fig. 13 and Fig. 14, the coefficients of determination (r^2) of the Langmuir isotherm for DR23 and AB92 onto the SEG adsorbent are higher than of Freundlich isotherm (Table 2). This suggests that the Freundlich model cannot describe well the adsorption process. By contrast, the Langmuir model can appropriately describe the adsorption of DR23 and AB92 onto the SEG

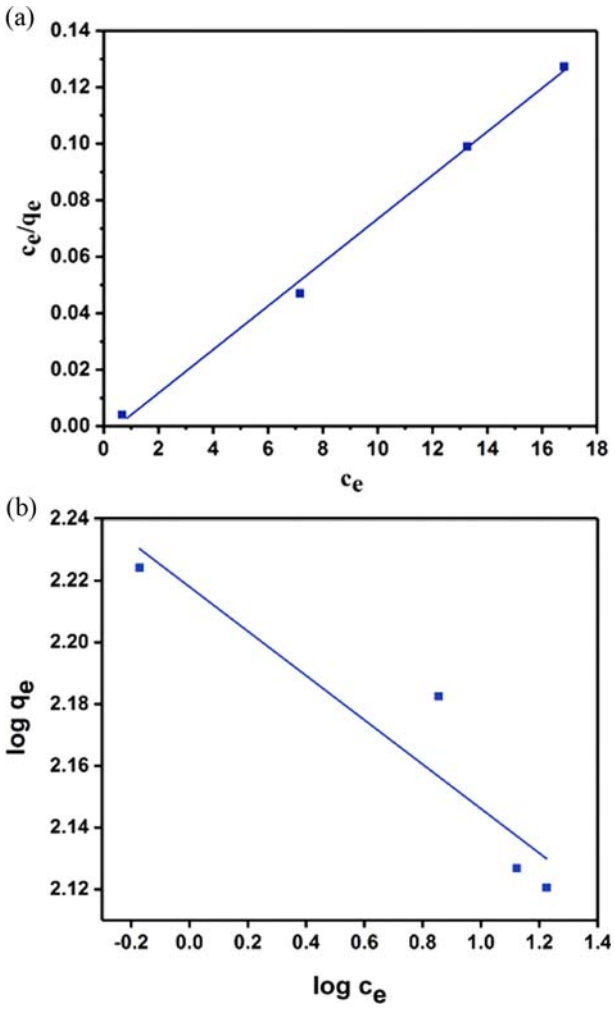

Fig. 13. Langmuir (a) and Freundlich (b) isotherm plots for the adsorption of DR23 (30 mg/L) onto SEG at pH of 2.19 and room temperature.

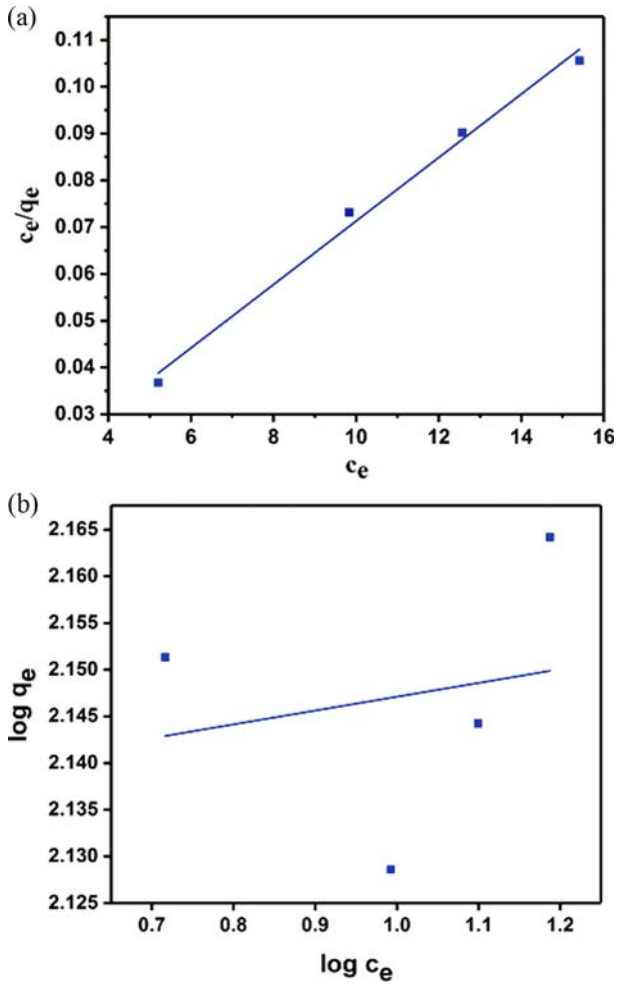

Fig. 14. Langmuir (a) and Freundlich (b) isotherm plots for the adsorption of AB92 (30 mg/L) onto SEG at pH of 2.16 and room temperature.

Table 2. Calculated quantities of the Langmuir and Freundlich models applied on DR23 and AB92 dyes

Sample	Langmuir				Freundlich		
	K_L (L/g)	q_m (mg/g)	R^2	R_L	k_f	n	R^2
DR23	2.081081081	129.8701299	0.9968	0.015764806	165.234222	13.9082058	0.8739
AB92	1.942857143	147.0588235	0.9921	0.01686747	135.6125867	67.56756757	0.0416

adsorbent. Armed with the separation factor (R_L) concept and its value calculated using Eq. (7), we can predict the adsorption of anionic dyes used in this work on the SEG adsorbent developed in this work, as follows:

$$R_L = \frac{1}{1+KC_0} \quad (7)$$

The quantity of R_L is a criterion suggesting the type of the isotherm to be favorable ($0<R_L<1$), unfavorable ($R_L>1$), linear ($R_L=1$) or irreversible ($R_L=0$) [46]. Based on this criterion and considering the separation factors calculated for SEG (Table 2), the adsorption of both DR23 and AB92 dyes on the SEG seems to be favorable.

CONCLUSION

This study assessed the ability of as-received and ethylenediamine/glutaraldehyde-modified starch (SEG), as a bioplatform, in removal of two kinds of industrial dyes from wastewater. The two anionic dyes used were AB92 and DR23, whose chemical structure is well-known. The cationic nature of starch surface was changed into an ionic structure after modification, where amine functional groups enabled effective removal of anionic dyes. The effects of adsorption parameters including initial dye concentration, adsorbent dosage and contact time on dye removal percent and adsorption capacity were thoroughly discussed. The prepared bioplatform led to a very high removal of anionic azo dyes (AB92 and DR23), that was 0.035 g per 1 g adsorbent. Changes in chemical structure of starch after modification with the assigned precursor were studied by FT-IR technique and FE-SEM, so that formation of new chemical bonds was signaled by new peaks in FT-IR spectra and ellipsoidal structure of starch changed into an amorphous irregular shape. Adsorption kinetics and adsorption isotherm models were applied and the kinetics of adsorption was fitted well by a pseudo-second-order kinetic model and Langmuir isotherm model, respectively. The results confirmed that SEG can be used for wastewater treatment as a biosorbent.

REFERENCES

1. N. M. Mahmoodi, *J. Environ. Eng.*, **139**, 1368 (2013).
2. N. M. Mahmoodi, *Desalin. Water Treat.*, **53**, 84 (2015).
3. N. M. Mahmoodi, M. Oveisi, A. Taghizadeh and M. Taghizadeh, *J. Hazard. Mater.*, **368**, 746 (2019).
4. N. M. Mahmoodi, J. Abdi and D. Bastani, *J. Environ. Health Sci. Eng.*, **12**, 96 (2014).
5. N. M. Mahmoodi, *J. Taiwan Inst. Chem. Eng.*, **45**, 2008 (2014).
6. N. M. Mahmoodi, *Water, Air, Soil Pollut.*, **224**, 1419 (2013).
7. A. Almasian, M. E. Olya and N. M. Mahmoodi, *J. Taiwan Inst. Chem. Eng.*, **49**, 119 (2015).
8. N. M. Mahmoodi, *Water, Air, Soil Pollut.*, **224**, 1612 (2013).
9. G. Liu, Z. Gu, Y. Hong, L. Cheng and C. Li, *Trends Food Sci. Technol.*, **63**, 70 (2017).
10. N. L. Vanier, S. L. M. El Halal, A. R. G. Dias and E. da Rosa Zavareze, *Food Chem.*, **221**, 1546 (2017).
11. O. Tavakoli, V. Goodarzi, M. R. Saeb, N. M. Mahmoodi and R. Borja, *J. Hazard. Mater.*, **334**, 256 (2017).
12. M. G. Sari, M. R. Saeb, M. Shabanian, M. Khaleghi, H. Vahabi, C. Vagner, P. Zarrintaj, R. Khalili, S. M. R. Paran, B. Ramezanzadeh and M. Mozafari, *Prog. Org. Coat.*, **115**, 143 (2018).
13. S. Van Vlierberghe, P. Dubruel and E. Schacht, *Biomacromolecules*, **12**, 1387 (2011).
14. P. Zarrintaj, S. Manouchehri, Z. Ahmadi, M. R. Saeb, A. M. Urbanska, D. L. Kaplan and M. Mozafari, *Carbohyd. Polym.*, **187**, 66 (2018).
15. P. Zarrintaj, A. S. Moghaddam, S. Manouchehri, Z. Atoufi, A. Amiri, M. A. Amirkhani, M. A. Nilforoushzadeh, M. R. Saeb, M. R. Hamblin and M. Mozafari, *Nanomedicine*, **12**, 2403 (2017).
16. P. Zarrintaj, A. M. Urbanska, S. S. Gholizadeh, V. Goodarzi, M. R. Saeb and M. Mozafari, *J. Colloid Interface Sci.*, **516**, 57 (2018).
17. M. A. Nilforoushzadeh, M. A. Amirkhani, P. Zarrintaj, A. Salehi Moghaddam, T. Mehrabi, S. Alavi and M. Mollapour Sisakht, *J. Cosm. Dermatol.*, **17**, 693 (2018).
18. D. Le Corre, J. Bras and A. Dufresne, *Biomacromolecules*, **11**, 1139 (2010).
19. S. F. Chin, S. C. Pang and S. H. Tay, *Carbohyd. Polym.*, **86**, 1817 (2011).
20. Y. Sugahara and T. Ohta, *J. Appl. Polym. Sci.*, **82**, 1437 (2001).
21. E. Yarahmadi, K. Didehban, M. G. Sari, M. R. Saeb, M. Shabanian, F. Aryanasab, P. Zarrintaj, S. M. R. Paran, M. Mozafari, M. Rallini and D. Puglia, *Prog. Org. Coat.*, **119**, 194 (2018).
22. I. Damager, S. B. Engelsen, A. Blennow, B. Lindberg Møller and M. S. Motawia, *Chem. Rev.*, **110**, 2049 (2010).
23. P. W. Gous and G. P. Fox, *Trend. Food Sci. Technol.*, **62**, 23 (2017).
24. F. Nazarian-Firouzabadi and R. G. Visser, *Biochem. Biophysics Rep.*, **10**, 7 (2017).
25. F. A. Ngwabebhoh, M. Gazi and A. A. Oladipo, *Chem. Eng. Res. Design*, **112**, 274 (2016).
26. M. Ganjaee Sari, H. Vahabi, X. Gabrion, P. Laheurte, P. Zarrintaj, K. Formela and M. R. Saeb, *Prog. Org. Coat.*, **119**, 171 (2018).
27. X. Liu and Q. Wei, *RSC Adv.*, **6**, 79853 (2016).
28. S. Mohebbi, M. N. Nezhad, P. Zarrintaj, S. H. Jafari, S. S. Gholizadeh, M. R. Saeb and M. Mozafari, *Curr. Stem Cell Res. Ther.*, **14**, 93 (2019).
29. S. Manouchehri, B. Bagheri, S. H. Rad, M. N. Nezhad, Y. C. Kim, O. O. Park, M. Farokhi, M. Jouyandeh, M. R. Ganjali, M. K. Yazdi,

P. Zarrintaj and M. R. Saeb, *Prog. Org. Coat.*, **131**, 389 (2019).
30. Z. Bagher, Z. Atoufi, R. Alizadeh, M. Farhadi, P. Zarrintaj, L. Moroni, M. Setayeshmehr, A. Komeili and S. K. Kamrava, *Mater. Sci. Eng. C*, **101**, 243 (2019).
31. G. Crini, *Prog. Polym. Sci.*, **30**, 38 (2005).
32. A. Pourjavadi, Z. M. Tehrani and S. H. Hosseini, *RSC Adv.*, **5**, 48586 (2015).
33. A. Zhang, Z. Zhang, F. Shi, J. Ding, C. Xiao, X. Zhuang, C. He, L. Chen and X. Chen, *Soft Matter*, **9**, 2224 (2013).
34. Q. Chen, H. Yu, L. Wang, Z. ul Abdin, Y. Chen, J. Wang, W. Zhou, X. Yang, R. U. Khan and H. Zhang, *RSC Adv.*, **5**, 67459 (2015).
35. D. Li, N. Yang, Y. Jin, L. Guo, Y. Zhou, Z. Xie, Z. Jin and X. Xu, *Food Chem.*, **229**, 57 (2017).
36. N. Masina, Y. E. Choonara, P. Kumar, L. C. du Toit, M. Govender, S. Indermun and V. Pillay, *Carbohyd. Polym.*, **157**, 1226 (2017).
37. E. S. Dragan and D. F. Apopei, *Chem. Eng. J.*, **178**, 252 (2011).
38. F. Gimbert, N. Morin-Crini, F. Renault, P.-M. Badot and G. Crini, *J. Hazard. Mater.*, **157**, 34 (2008).
39. S. Xu, J. Wang, R. Wu, J. Wang and H. Li, *Chem. Eng. J.*, **117**, 161 (2006).
40. N. M. Mahmoodi, B. Hayati, M. Arami and C. Lan, *Desalination*, **268**, 117 (2011).
41. A. Tehrani-Bagha, N. Mahmoodi and F. Menger, *Desalination*, **260**, 34 (2010).
42. E. Daneshvar, A. Vazirzadeh, A. Niazi, M. Kousha, M. Naushad and A. Bhatnagar, *J. Clean. Prod.*, **152**, 443 (2017).
43. M. T. Yagub, T. K. Sen, S. Afroze and H. M. Ang, *Adv. Colloid Interface Sci.*, **209**, 172 (2014).
44. L. Liu, Y. Wan, Y. Xie, R. Zhai, B. Zhang and J. Liu, *Chem. Eng. J.*, **187**, 210 (2012).
45. R. Cheng, S. Ou, M. Li, Y. Li and B. Xiang, *J. Hazard. Mater.*, **172**, 1665 (2009).
46. R. F. Gomes, A. C. N. de Azevedo, A. G. Pereira, E. C. Muniz, A. R. Fajardo and F. H. Rodrigues, *J. Colloid Interface Sci.*, **454**, 200 (2015).
47. J. R. Ferraro and L. J. Basile, Fourier transform infrared spectra: applications to chemical systems, Elsevier, Amsterdam, Netherlands (2012).
48. M. Naushad, T. Ahamad, G. Sharma, H. Ala'a, A. B. Albadarin, M. M. Alam, Z. A. ALOthman, S. M. Alshehri and A. A. Ghfar, *Chem. Eng. J.*, **300**, 306 (2016).
49. D. L. Pavia, G. M. Lampman and G. S. Kriz, Introduction to Spectroscopy: a guide for students of organic chemistry. 1979, Fort Worth, Texas (2009).
50. P. Luo, B. Zhang, Y. Zhao, J. Wang, H. Zhang and J. Liu, *Korean J. Chem. Eng.*, **28**, 800 (2011).
51. V. V. Panić, S. I. Šešlija, A. R. Nešić and S. J. Veličković, *Hemijska Industrija*, **67**, 881 (2013).
52. N. D. Tumin, A. L. Chuah, Z. Zawani and S. A. Rashid, *J. Eng. Sci. Technol.*, **3**, 180 (2008).
53. C. W. Chiu and D. Solarek, *Starch Chem. Technol.*, **3**, 629 (2009).
54. F. Hosseini, S. Sadighian, H. Hosseini-Monfared and N. M. Mahmoodi, *Desalin. Water Treat.*, **57**, 24378 (2016).
55. A. Erdem, F. A. Ngwabebhoh and U. Yildiz, *J. Environ. Chem. Eng.*, **5**, 1269 (2017).
56. S. N. Jain, Z. Shaikh, V. S. Mane, S. Vishnoi, V. N. Mawal, O. R. Patel, P. S. Bhandari and M. S. Gaikwad, *Microchem. J.*, **148**, 605 (2019).
57. G. Gong, F. Zhang, Z. Cheng and L. Zhou, *Int. J. Biol. Macromol.*, **81**, 205 (2015).